CONTINUOUS CONTROL WITH DEEP REINFORCEMENT LEARNING

Timothy P. Lillicrap*, Jonathan J. Hunt*, Alexander Pritzel, Nicolas Heess,
Tom Erez, Yuval Tassa, David Silver & Daan Wierstra
Google Deepmind
London, UK
{countzero, jjhunt, apritzel, heess,
etom, tassa, davidsilver, wierstra} @ google.com

arXiv:1509.02971v6 [cs.LG] 5 Jul 2019

ABSTRACT

We adapt the ideas underlying the success of Deep Q-Learning to the continuous action domain. We present an actor-critic, model-free algorithm based on the deterministic policy gradient that can operate over continuous action spaces. Using the same learning algorithm, network architecture and hyper-parameters, our algorithm robustly solves more than 20 simulated physics tasks, including classic problems such as cartpole swing-up, dexterous manipulation, legged locomotion and car driving. Our algorithm is able to find policies whose performance is competitive with those found by a planning algorithm with full access to the dynamics of the domain and its derivatives. We further demonstrate that for many of the tasks the algorithm can learn policies "end-to-end": directly from raw pixel inputs.

1 INTRODUCTION

One of the primary goals of the field of artificial intelligence is to solve complex tasks from unprocessed, high-dimensional, sensory input. Recently, significant progress has been made by combining advances in deep learning for sensory processing (Krizhevsky et al., 2012) with reinforcement learning, resulting in the "Deep Q Network" (DQN) algorithm (Mnih et al., 2015) that is capable of human level performance on many Atari video games using unprocessed pixels for input. To do so, deep neural network function approximators were used to estimate the action-value function.

However, while DQN solves problems with high-dimensional observation spaces, it can only handle discrete and low-dimensional action spaces. Many tasks of interest, most notably physical control tasks, have continuous (real valued) and high dimensional action spaces. DQN cannot be straightforwardly applied to continuous domains since it relies on a finding the action that maximizes the action-value function, which in the continuous valued case requires an iterative optimization process at every step.

An obvious approach to adapting deep reinforcement learning methods such as DQN to continuous domains is to to simply discretize the action space. However, this has many limitations, most notably the curse of dimensionality: the number of actions increases exponentially with the number of degrees of freedom. For example, a 7 degree of freedom system (as in the human arm) with the coarsest discretization $a_i \in \{-k, 0, k\}$ for each joint leads to an action space with dimensionality: $3^7 = 2187$. The situation is even worse for tasks that require fine control of actions as they require a correspondingly finer grained discretization, leading to an explosion of the number of discrete actions. Such large action spaces are difficult to explore efficiently, and thus successfully training DQN-like networks in this context is likely intractable. Additionally, naive discretization of action spaces needlessly throws away information about the structure of the action domain, which may be essential for solving many problems.

In this work we present a model-free, off-policy actor-critic algorithm using deep function approximators that can learn policies in high-dimensional, continuous action spaces. Our work is based

*These authors contributed equally.

on the deterministic policy gradient (DPG) algorithm (Silver et al., 2014) (itself similar to NFQCA (Hafner & Riedmiller, 2011), and similar ideas can be found in (Prokhorov et al., 1997)). However, as we show below, a naive application of this actor-critic method with neural function approximators is unstable for challenging problems.

Here we combine the actor-critic approach with insights from the recent success of Deep Q Network (DQN) (Mnih et al., 2013; 2015). Prior to DQN, it was generally believed that learning value functions using large, non-linear function approximators was difficult and unstable. DQN is able to learn value functions using such function approximators in a stable and robust way due to two innovations: 1. the network is trained off-policy with samples from a replay buffer to minimize correlations between samples; 2. the network is trained with a target Q network to give consistent targets during temporal difference backups. In this work we make use of the same ideas, along with batch normalization (Ioffe & Szegedy, 2015), a recent advance in deep learning.

In order to evaluate our method we constructed a variety of challenging physical control problems that involve complex multi-joint movements, unstable and rich contact dynamics, and gait behavior. Among these are classic problems such as the cartpole swing-up problem, as well as many new domains. A long-standing challenge of robotic control is to learn an action policy directly from raw sensory input such as video. Accordingly, we place a fixed viewpoint camera in the simulator and attempted all tasks using both low-dimensional observations (e.g. joint angles) and directly from pixels.

Our model-free approach which we call Deep DPG (DDPG) can learn competitive policies for all of our tasks using low-dimensional observations (e.g. cartesian coordinates or joint angles) using the same hyper-parameters and network structure. In many cases, we are also able to learn good policies directly from pixels, again keeping hyperparameters and network structure constant [1].

A key feature of the approach is its simplicity: it requires only a straightforward actor-critic architecture and learning algorithm with very few "moving parts", making it easy to implement and scale to more difficult problems and larger networks. For the physical control problems we compare our results to a baseline computed by a planner (Tassa et al., 2012) that has full access to the underlying simulated dynamics and its derivatives (see supplementary information). Interestingly, DDPG can sometimes find policies that exceed the performance of the planner, in some cases even when learning from pixels (the planner always plans over the underlying low-dimensional state space).

2 BACKGROUND

We consider a standard reinforcement learning setup consisting of an agent interacting with an environment E in discrete timesteps. At each timestep t the agent receives an observation x_t, takes an action a_t and receives a scalar reward r_t. In all the environments considered here the actions are real-valued $a_t \in \mathbb{R}^N$. In general, the environment may be partially observed so that the entire history of the observation, action pairs $s_t = (x_1, a_1, ..., a_{t-1}, x_t)$ may be required to describe the state. Here, we assumed the environment is fully-observed so $s_t = x_t$.

An agent's behavior is defined by a policy, π, which maps states to a probability distribution over the actions $\pi: \mathcal{S} \rightarrow \mathcal{P}(\mathcal{A})$. The environment, E, may also be stochastic. We model it as a Markov decision process with a state space $\mathcal{S}$, action space $\mathcal{A} = \mathbb{R}^N$, an initial state distribution $p(s_1)$, transition dynamics $p(s_{t+1}|s_t, a_t)$, and reward function $r(s_t, a_t)$.

The return from a state is defined as the sum of discounted future reward $R_t = \sum_{i=t}^{T} \gamma^{(i-t)} r(s_i, a_i)$ with a discounting factor $\gamma \in [0, 1]$. Note that the return depends on the actions chosen, and therefore on the policy π, and may be stochastic. The goal in reinforcement learning is to learn a policy which maximizes the expected return from the start distribution $J = \mathbb{E}_{r_i, s_i \sim E, a_i \sim \pi}[R_1]$. We denote the discounted state visitation distribution for a policy π as ρ^π.

The action-value function is used in many reinforcement learning algorithms. It describes the expected return after taking an action a_t in state s_t and thereafter following policy π:

$$Q^\pi(s_t, a_t) = \mathbb{E}_{r_{i \geq t}, s_{i>t} \sim E, a_{i>t} \sim \pi}[R_t | s_t, a_t] \tag{1}$$

[1] You can view a movie of some of the learned policies at `https://goo.gl/J4PIAz`

Many approaches in reinforcement learning make use of the recursive relationship known as the Bellman equation:

$$Q^\pi(s_t, a_t) = \mathbb{E}_{r_t, s_{t+1} \sim E}\left[r(s_t, a_t) + \gamma\, \mathbb{E}_{a_{t+1} \sim \pi}\left[Q^\pi(s_{t+1}, a_{t+1})\right]\right] \tag{2}$$

If the target policy is deterministic we can describe it as a function $\mu : \mathcal{S} \leftarrow \mathcal{A}$ and avoid the inner expectation:

$$Q^\mu(s_t, a_t) = \mathbb{E}_{r_t, s_{t+1} \sim E}\left[r(s_t, a_t) + \gamma Q^\mu(s_{t+1}, \mu(s_{t+1}))\right] \tag{3}$$

The expectation depends only on the environment. This means that it is possible to learn Q^μ off-policy, using transitions which are generated from a different stochastic behavior policy β.

Q-learning (Watkins & Dayan, 1992), a commonly used off-policy algorithm, uses the greedy policy $\mu(s) = \arg\max_a Q(s, a)$. We consider function approximators parameterized by θ^Q, which we optimize by minimizing the loss:

$$L(\theta^Q) = \mathbb{E}_{s_t \sim \rho^\beta, a_t \sim \beta, r_t \sim E}\left[\left(Q(s_t, a_t|\theta^Q) - y_t\right)^2\right] \tag{4}$$

where

$$y_t = r(s_t, a_t) + \gamma Q(s_{t+1}, \mu(s_{t+1})|\theta^Q). \tag{5}$$

While y_t is also dependent on θ^Q, this is typically ignored.

The use of large, non-linear function approximators for learning value or action-value functions has often been avoided in the past since theoretical performance guarantees are impossible, and practically learning tends to be unstable. Recently, (Mnih et al., 2013; 2015) adapted the Q-learning algorithm in order to make effective use of large neural networks as function approximators. Their algorithm was able to learn to play Atari games from pixels. In order to scale Q-learning they introduced two major changes: the use of a *replay buffer*, and a separate *target network* for calculating y_t. We employ these in the context of DDPG and explain their implementation in the next section.

3 ALGORITHM

It is not possible to straightforwardly apply Q-learning to continuous action spaces, because in continuous spaces finding the greedy policy requires an optimization of a_t at every timestep; this optimization is too slow to be practical with large, unconstrained function approximators and nontrivial action spaces. Instead, here we used an actor-critic approach based on the DPG algorithm (Silver et al., 2014).

The DPG algorithm maintains a parameterized actor function $\mu(s|\theta^\mu)$ which specifies the current policy by deterministically mapping states to a specific action. The critic $Q(s, a)$ is learned using the Bellman equation as in Q-learning. The actor is updated by following the applying the chain rule to the expected return from the start distribution J with respect to the actor parameters:

$$\begin{aligned} \nabla_{\theta^\mu} J &\approx \mathbb{E}_{s_t \sim \rho^\beta}\left[\nabla_{\theta^\mu} Q(s, a|\theta^Q)|_{s=s_t, a=\mu(s_t|\theta^\mu)}\right] \\ &= \mathbb{E}_{s_t \sim \rho^\beta}\left[\nabla_a Q(s, a|\theta^Q)|_{s=s_t, a=\mu(s_t)} \nabla_{\theta_\mu} \mu(s|\theta^\mu)|_{s=s_t}\right] \end{aligned} \tag{6}$$

Silver et al. (2014) proved that this is the *policy gradient*, the gradient of the policy's performance [2].

As with Q learning, introducing non-linear function approximators means that convergence is no longer guaranteed. However, such approximators appear essential in order to learn and generalize on large state spaces. NFQCA (Hafner & Riedmiller, 2011), which uses the same update rules as DPG but with neural network function approximators, uses batch learning for stability, which is intractable for large networks. A minibatch version of NFQCA which does not reset the policy at each update, as would be required to scale to large networks, is equivalent to the original DPG, which we compare to here. Our contribution here is to provide modifications to DPG, inspired by the success of DQN, which allow it to use neural network function approximators to learn in large state and action spaces online. We refer to our algorithm as Deep DPG (DDPG, Algorithm 1).

[2] In practice, as in commonly done in policy gradient implementations, we ignored the discount in the state-visitation distribution ρ^β.

One challenge when using neural networks for reinforcement learning is that most optimization algorithms assume that the samples are independently and identically distributed. Obviously, when the samples are generated from exploring sequentially in an environment this assumption no longer holds. Additionally, to make efficient use of hardware optimizations, it is essential to learn in minibatches, rather than online.

As in DQN, we used a replay buffer to address these issues. The replay buffer is a finite sized cache $\mathcal{R}$. Transitions were sampled from the environment according to the exploration policy and the tuple (s_t, a_t, r_t, s_{t+1}) was stored in the replay buffer. When the replay buffer was full the oldest samples were discarded. At each timestep the actor and critic are updated by sampling a minibatch uniformly from the buffer. Because DDPG is an off-policy algorithm, the replay buffer can be large, allowing the algorithm to benefit from learning across a set of uncorrelated transitions.

Directly implementing Q learning (equation 4) with neural networks proved to be unstable in many environments. Since the network $Q(s, a|\theta^Q)$ being updated is also used in calculating the target value (equation 5), the Q update is prone to divergence. Our solution is similar to the target network used in (Mnih et al., 2013) but modified for actor-critic and using "soft" target updates, rather than directly copying the weights. We create a copy of the actor and critic networks, $Q'(s, a|\theta^{Q'})$ and $\mu'(s|\theta^{\mu'})$ respectively, that are used for calculating the target values. The weights of these target networks are then updated by having them slowly track the learned networks: $\theta' \leftarrow \tau\theta + (1 - \tau)\theta'$ with $\tau \ll 1$. This means that the target values are constrained to change slowly, greatly improving the stability of learning. This simple change moves the relatively unstable problem of learning the action-value function closer to the case of supervised learning, a problem for which robust solutions exist. We found that having both a target μ' and Q' was required to have stable targets y_i in order to consistently train the critic without divergence. This may slow learning, since the target network delays the propagation of value estimations. However, in practice we found this was greatly outweighed by the stability of learning.

When learning from low dimensional feature vector observations, the different components of the observation may have different physical units (for example, positions versus velocities) and the ranges may vary across environments. This can make it difficult for the network to learn effectively and may make it difficult to find hyper-parameters which generalise across environments with different scales of state values.

One approach to this problem is to manually scale the features so they are in similar ranges across environments and units. We address this issue by adapting a recent technique from deep learning called *batch normalization* (Ioffe & Szegedy, 2015). This technique normalizes each dimension across the samples in a minibatch to have unit mean and variance. In addition, it maintains a running average of the mean and variance to use for normalization during testing (in our case, during exploration or evaluation). In deep networks, it is used to minimize covariance shift during training, by ensuring that each layer receives whitened input. In the low-dimensional case, we used batch normalization on the state input and all layers of the μ network and all layers of the Q network prior to the action input (details of the networks are given in the supplementary material). With batch normalization, we were able to learn effectively across many different tasks with differing types of units, without needing to manually ensure the units were within a set range.

A major challenge of learning in continuous action spaces is exploration. An advantage of off-policies algorithms such as DDPG is that we can treat the problem of exploration independently from the learning algorithm. We constructed an exploration policy μ' by adding noise sampled from a noise process $\mathcal{N}$ to our actor policy

$$\mu'(s_t) = \mu(s_t|\theta_t^\mu) + \mathcal{N} \tag{7}$$

$\mathcal{N}$ can be chosen to suit the environment. As detailed in the supplementary materials we used an Ornstein-Uhlenbeck process (Uhlenbeck & Ornstein, 1930) to generate temporally correlated exploration for exploration efficiency in physical control problems with inertia (similar use of auto-correlated noise was introduced in (Wawrzyński, 2015)).

4 RESULTS

We constructed simulated physical environments of varying levels of difficulty to test our algorithm. This included classic reinforcement learning environments such as cartpole, as well as difficult,

Algorithm 1 DDPG algorithm

Randomly initialize critic network $Q(s, a|\theta^Q)$ and actor $\mu(s|\theta^\mu)$ with weights θ^Q and θ^μ.
Initialize target network Q' and μ' with weights $\theta^{Q'} \leftarrow \theta^Q$, $\theta^{\mu'} \leftarrow \theta^\mu$
Initialize replay buffer R
for episode = 1, M **do**
  Initialize a random process $\mathcal{N}$ for action exploration
  Receive initial observation state s_1
  for t = 1, T **do**
    Select action $a_t = \mu(s_t|\theta^\mu) + \mathcal{N}_t$ according to the current policy and exploration noise
    Execute action a_t and observe reward r_t and observe new state s_{t+1}
    Store transition (s_t, a_t, r_t, s_{t+1}) in R
    Sample a random minibatch of N transitions (s_i, a_i, r_i, s_{i+1}) from R
    Set $y_i = r_i + \gamma Q'(s_{i+1}, \mu'(s_{i+1}|\theta^{\mu'})|\theta^{Q'})$
    Update critic by minimizing the loss: $L = \frac{1}{N}\sum_i (y_i - Q(s_i, a_i|\theta^Q))^2$
    Update the actor policy using the sampled policy gradient:

$$\nabla_{\theta^\mu} J \approx \frac{1}{N} \sum_i \nabla_a Q(s, a|\theta^Q)|_{s=s_i, a=\mu(s_i)} \nabla_{\theta^\mu} \mu(s|\theta^\mu)|_{s_i}$$

    Update the target networks:

$$\theta^{Q'} \leftarrow \tau\theta^Q + (1-\tau)\theta^{Q'}$$
$$\theta^{\mu'} \leftarrow \tau\theta^\mu + (1-\tau)\theta^{\mu'}$$

  end for
end for

high dimensional tasks such as gripper, tasks involving contacts such as puck striking (*canada*) and locomotion tasks such as *cheetah* (Wawrzyński, 2009). In all domains but *cheetah* the actions were torques applied to the actuated joints. These environments were simulated using MuJoCo (Todorov et al., 2012). Figure 1 shows renderings of some of the environments used in the task (the supplementary contains details of the environments and you can view some of the learned policies at `https://goo.gl/J4PIAz`).

In all tasks, we ran experiments using both a low-dimensional state description (such as joint angles and positions) and high-dimensional renderings of the environment. As in DQN (Mnih et al., 2013; 2015), in order to make the problems approximately fully observable in the high dimensional environment we used action repeats. For each timestep of the agent, we step the simulation 3 timesteps, repeating the agent's action and rendering each time. Thus the observation reported to the agent contains 9 feature maps (the RGB of each of the 3 renderings) which allows the agent to infer velocities using the differences between frames. The frames were downsampled to 64x64 pixels and the 8-bit RGB values were converted to floating point scaled to $[0, 1]$. See supplementary information for details of our network structure and hyperparameters.

We evaluated the policy periodically during training by testing it without exploration noise. Figure 2 shows the performance curve for a selection of environments. We also report results with components of our algorithm (i.e. the target network or batch normalization) removed. In order to perform well across all tasks, both of these additions are necessary. In particular, learning without a target network, as in the original work with DPG, is very poor in many environments.

Surprisingly, in some simpler tasks, learning policies from pixels is just as fast as learning using the low-dimensional state descriptor. This may be due to the action repeats making the problem simpler. It may also be that the convolutional layers provide an easily separable representation of state space, which is straightforward for the higher layers to learn on quickly.

Table 1 summarizes DDPG's performance across all of the environments (results are averaged over 5 replicas). We normalized the scores using two baselines. The first baseline is the mean return from a naive policy which samples actions from a uniform distribution over the valid action space. The second baseline is iLQG (Todorov & Li, 2005), a planning based solver with full access to the

underlying physical model and its derivatives. We normalize scores so that the naive policy has a mean score of 0 and iLQG has a mean score of 1. DDPG is able to learn good policies on many of the tasks, and in many cases some of the replicas learn policies which are superior to those found by iLQG, even when learning directly from pixels.

It can be challenging to learn accurate value estimates. Q-learning, for example, is prone to over-estimating values (Hasselt, 2010). We examined DDPG's estimates empirically by comparing the values estimated by Q after training with the true returns seen on test episodes. Figure 3 shows that in simple tasks DDPG estimates returns accurately without systematic biases. For harder tasks the Q estimates are worse, but DDPG is still able learn good policies.

To demonstrate the generality of our approach we also include Torcs, a racing game where the actions are acceleration, braking and steering. Torcs has previously been used as a testbed in other policy learning approaches (Koutník et al., 2014b). We used an identical network architecture and learning algorithm hyper-parameters to the physics tasks but altered the noise process for exploration because of the very different time scales involved. On both low-dimensional and from pixels, some replicas were able to learn reasonable policies that are able to complete a circuit around the track though other replicas failed to learn a sensible policy.

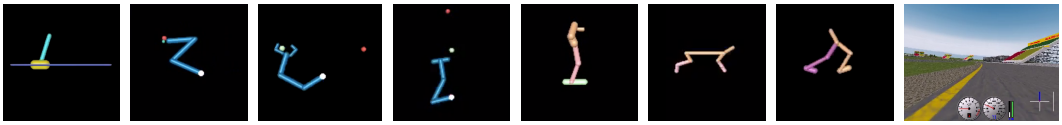

Figure 1: Example screenshots of a sample of environments we attempt to solve with DDPG. In order from the left: the cartpole swing-up task, a reaching task, a gasp and move task, a puck-hitting task, a monoped balancing task, two locomotion tasks and Torcs (driving simulator). We tackle all tasks using both low-dimensional feature vector and high-dimensional pixel inputs. Detailed descriptions of the environments are provided in the supplementary. Movies of some of the learned policies are available at `https://goo.gl/J4PIAz`.

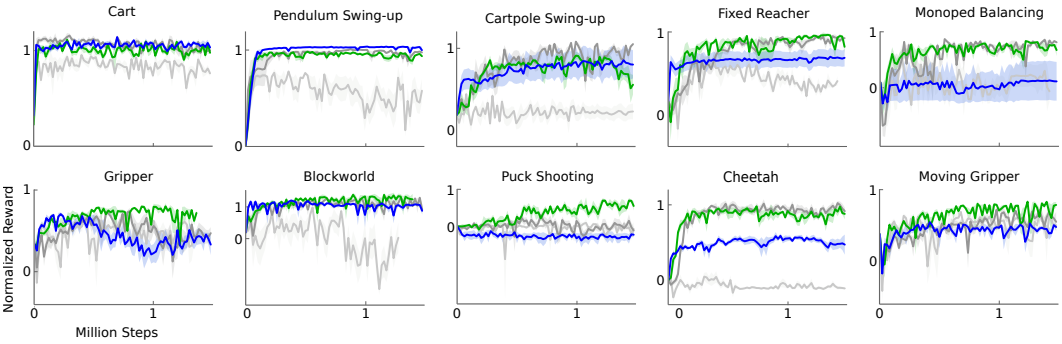

Figure 2: Performance curves for a selection of domains using variants of DPG: original DPG algorithm (minibatch NFQCA) with batch normalization (light grey), with target network (dark grey), with target networks and batch normalization (green), with target networks from pixel-only inputs (blue). Target networks are crucial.

5 Related work

The original DPG paper evaluated the algorithm with toy problems using tile-coding and linear function approximators. It demonstrated data efficiency advantages for off-policy DPG over both on- and off-policy stochastic actor critic. It also solved one more challenging task in which a multi-jointed octopus arm had to strike a target with any part of the limb. However, that paper did not demonstrate scaling the approach to large, high-dimensional observation spaces as we have here.

It has often been assumed that standard policy search methods such as those explored in the present work are simply too fragile to scale to difficult problems (Levine et al., 2015). Standard policy search

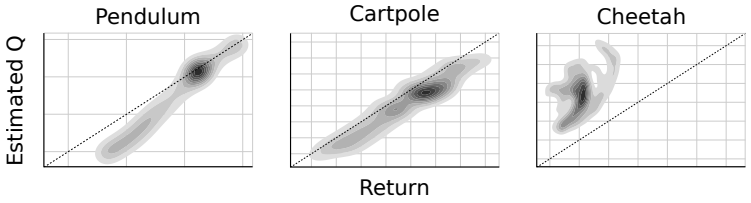

Figure 3: Density plot showing estimated Q values versus observed returns sampled from test episodes on 5 replicas. In simple domains such as pendulum and cartpole the Q values are quite accurate. In more complex tasks, the Q estimates are less accurate, but can still be used to learn competent policies. Dotted line indicates unity, units are arbitrary.

Table 1: Performance after training across all environments for at most 2.5 million steps. We report both the average and best observed (across 5 runs). All scores, except Torcs, are normalized so that a random agent receives 0 and a planning algorithm 1; for Torcs we present the raw reward score. We include results from the DDPG algorithn in the low-dimensional ($lowd$) version of the environment and high-dimensional (pix). For comparision we also include results from the original DPG algorithm with a replay buffer and batch normalization ($cntrl$).

environment	$R_{av,lowd}$	$R_{best,lowd}$	$R_{av,pix}$	$R_{best,pix}$	$R_{av,cntrl}$	$R_{best,cntrl}$
blockworld1	1.156	1.511	0.466	1.299	-0.080	1.260
blockworld3da	0.340	0.705	0.889	2.225	-0.139	0.658
canada	0.303	1.735	0.176	0.688	0.125	1.157
canada2d	0.400	0.978	-0.285	0.119	-0.045	0.701
cart	0.938	1.336	1.096	1.258	0.343	1.216
cartpole	0.844	1.115	0.482	1.138	0.244	0.755
cartpoleBalance	0.951	1.000	0.335	0.996	-0.468	0.528
cartpoleParallelDouble	0.549	0.900	0.188	0.323	0.197	0.572
cartpoleSerialDouble	0.272	0.719	0.195	0.642	0.143	0.701
cartpoleSerialTriple	0.736	0.946	0.412	0.427	0.583	0.942
cheetah	0.903	1.206	0.457	0.792	-0.008	0.425
fixedReacher	0.849	1.021	0.693	0.981	0.259	0.927
fixedReacherDouble	0.924	0.996	0.872	0.943	0.290	0.995
fixedReacherSingle	0.954	1.000	0.827	0.995	0.620	0.999
gripper	0.655	0.972	0.406	0.790	0.461	0.816
gripperRandom	0.618	0.937	0.082	0.791	0.557	0.808
hardCheetah	1.311	1.990	1.204	1.431	-0.031	1.411
hopper	0.676	0.936	0.112	0.924	0.078	0.917
hyq	0.416	0.722	0.234	0.672	0.198	0.618
movingGripper	0.474	0.936	0.480	0.644	0.416	0.805
pendulum	0.946	1.021	0.663	1.055	0.099	0.951
reacher	0.720	0.987	0.194	0.878	0.231	0.953
reacher3daFixedTarget	0.585	0.943	0.453	0.922	0.204	0.631
reacher3daRandomTarget	0.467	0.739	0.374	0.735	-0.046	0.158
reacherSingle	0.981	1.102	1.000	1.083	1.010	1.083
walker2d	0.705	1.573	0.944	1.476	0.393	1.397
torcs	-393.385	1840.036	-401.911	1876.284	-911.034	1961.600

is thought to be difficult because it deals simultaneously with complex environmental dynamics and a complex policy. Indeed, most past work with actor-critic and policy optimization approaches have had difficulty scaling up to more challenging problems (Deisenroth et al., 2013). Typically, this is due to instability in learning wherein progress on a problem is either destroyed by subsequent learning updates, or else learning is too slow to be practical.

Recent work with model-free policy search has demonstrated that it may not be as fragile as previously supposed. Wawrzyński (2009); Wawrzyński & Tanwani (2013) has trained stochastic policies

in an actor-critic framework with a replay buffer. Concurrent with our work, Balduzzi & Ghifary (2015) extended the DPG algorithm with a "deviator" network which explicitly learns $\partial Q/\partial a$. However, they only train on two low-dimensional domains. Heess et al. (2015) introduced SVG(0) which also uses a Q-critic but learns a stochastic policy. DPG can be considered the deterministic limit of SVG(0). The techniques we described here for scaling DPG are also applicable to stochastic policies by using the reparametrization trick (Heess et al., 2015; Schulman et al., 2015a).

Another approach, trust region policy optimization (TRPO) (Schulman et al., 2015b), directly constructs stochastic neural network policies without decomposing problems into optimal control and supervised phases. This method produces near monotonic improvements in return by making carefully chosen updates to the policy parameters, constraining updates to prevent the new policy from diverging too far from the existing policy. This approach does not require learning an action-value function, and (perhaps as a result) appears to be significantly less data efficient.

To combat the challenges of the actor-critic approach, recent work with guided policy search (GPS) algorithms (e.g., (Levine et al., 2015)) decomposes the problem into three phases that are relatively easy to solve: first, it uses full-state observations to create locally-linear approximations of the dynamics around one or more nominal trajectories, and then uses optimal control to find the locally-linear optimal policy along these trajectories; finally, it uses supervised learning to train a complex, non-linear policy (e.g. a deep neural network) to reproduce the state-to-action mapping of the optimized trajectories.

This approach has several benefits, including data efficiency, and has been applied successfully to a variety of real-world robotic manipulation tasks using vision. In these tasks GPS uses a similar convolutional policy network to ours with 2 notable exceptions: 1. it uses a spatial softmax to reduce the dimensionality of visual features into a single (x, y) coordinate for each feature map, and 2. the policy also receives direct low-dimensional state information about the configuration of the robot at the first fully connected layer in the network. Both likely increase the power and data efficiency of the algorithm and could easily be exploited within the DDPG framework.

PILCO (Deisenroth & Rasmussen, 2011) uses Gaussian processes to learn a non-parametric, probabilistic model of the dynamics. Using this learned model, PILCO calculates analytic policy gradients and achieves impressive data efficiency in a number of control problems. However, due to the high computational demand, PILCO is "impractical for high-dimensional problems" (Wahlström et al., 2015). It seems that deep function approximators are the most promising approach for scaling reinforcement learning to large, high-dimensional domains.

Wahlström et al. (2015) used a deep dynamical model network along with model predictive control to solve the pendulum swing-up task from pixel input. They trained a differentiable forward model and encoded the goal state into the learned latent space. They use model-predictive control over the learned model to find a policy for reaching the target. However, this approach is only applicable to domains with goal states that can be demonstrated to the algorithm.

Recently, evolutionary approaches have been used to learn competitive policies for Torcs from pixels using compressed weight parametrizations (Koutník et al., 2014a) or unsupervised learning (Koutník et al., 2014b) to reduce the dimensionality of the evolved weights. It is unclear how well these approaches generalize to other problems.

6 Conclusion

The work combines insights from recent advances in deep learning and reinforcement learning, resulting in an algorithm that robustly solves challenging problems across a variety of domains with continuous action spaces, even when using raw pixels for observations. As with most reinforcement learning algorithms, the use of non-linear function approximators nullifies any convergence guarantees; however, our experimental results demonstrate that stable learning without the need for any modifications between environments.

Interestingly, all of our experiments used substantially fewer steps of experience than was used by DQN learning to find solutions in the Atari domain. Nearly all of the problems we looked at were solved within 2.5 million steps of experience (and usually far fewer), a factor of 20 fewer steps than

DQN requires for good Atari solutions. This suggests that, given more simulation time, DDPG may solve even more difficult problems than those considered here.

A few limitations to our approach remain. Most notably, as with most model-free reinforcement approaches, DDPG requires a large number of training episodes to find solutions. However, we believe that a robust model-free approach may be an important component of larger systems which may attack these limitations (Gläscher et al., 2010).

REFERENCES

Balduzzi, David and Ghifary, Muhammad. Compatible value gradients for reinforcement learning of continuous deep policies. *arXiv preprint arXiv:1509.03005*, 2015.

Deisenroth, Marc and Rasmussen, Carl E. Pilco: A model-based and data-efficient approach to policy search. In *Proceedings of the 28th International Conference on machine learning (ICML-11)*, pp. 465–472, 2011.

Deisenroth, Marc Peter, Neumann, Gerhard, Peters, Jan, et al. A survey on policy search for robotics. *Foundations and Trends in Robotics*, 2(1-2):1–142, 2013.

Gläscher, Jan, Daw, Nathaniel, Dayan, Peter, and O'Doherty, John P. States versus rewards: dissociable neural prediction error signals underlying model-based and model-free reinforcement learning. *Neuron*, 66(4):585–595, 2010.

Glorot, Xavier, Bordes, Antoine, and Bengio, Yoshua. Deep sparse rectifier networks. In *Proceedings of the 14th International Conference on Artificial Intelligence and Statistics. JMLR W&CP Volume*, volume 15, pp. 315–323, 2011.

Hafner, Roland and Riedmiller, Martin. Reinforcement learning in feedback control. *Machine learning*, 84(1-2):137–169, 2011.

Hasselt, Hado V. Double q-learning. In *Advances in Neural Information Processing Systems*, pp. 2613–2621, 2010.

Heess, N., Hunt, J. J, Lillicrap, T. P, and Silver, D. Memory-based control with recurrent neural networks. *NIPS Deep Reinforcement Learning Workshop (arXiv:1512.04455)*, 2015.

Heess, Nicolas, Wayne, Gregory, Silver, David, Lillicrap, Tim, Erez, Tom, and Tassa, Yuval. Learning continuous control policies by stochastic value gradients. In *Advances in Neural Information Processing Systems*, pp. 2926–2934, 2015.

Ioffe, Sergey and Szegedy, Christian. Batch normalization: Accelerating deep network training by reducing internal covariate shift. *arXiv preprint arXiv:1502.03167*, 2015.

Kingma, Diederik and Ba, Jimmy. Adam: A method for stochastic optimization. *arXiv preprint arXiv:1412.6980*, 2014.

Koutník, Jan, Schmidhuber, Jürgen, and Gomez, Faustino. Evolving deep unsupervised convolutional networks for vision-based reinforcement learning. In *Proceedings of the 2014 conference on Genetic and evolutionary computation*, pp. 541–548. ACM, 2014a.

Koutník, Jan, Schmidhuber, Jürgen, and Gomez, Faustino. Online evolution of deep convolutional network for vision-based reinforcement learning. In *From Animals to Animats 13*, pp. 260–269. Springer, 2014b.

Krizhevsky, Alex, Sutskever, Ilya, and Hinton, Geoffrey E. Imagenet classification with deep convolutional neural networks. In *Advances in neural information processing systems*, pp. 1097–1105, 2012.

Levine, Sergey, Finn, Chelsea, Darrell, Trevor, and Abbeel, Pieter. End-to-end training of deep visuomotor policies. *arXiv preprint arXiv:1504.00702*, 2015.

Mnih, Volodymyr, Kavukcuoglu, Koray, Silver, David, Graves, Alex, Antonoglou, Ioannis, Wierstra, Daan, and Riedmiller, Martin. Playing atari with deep reinforcement learning. *arXiv preprint arXiv:1312.5602*, 2013.

Mnih, Volodymyr, Kavukcuoglu, Koray, Silver, David, Rusu, Andrei A, Veness, Joel, Bellemare, Marc G, Graves, Alex, Riedmiller, Martin, Fidjeland, Andreas K, Ostrovski, Georg, et al. Human-level control through deep reinforcement learning. *Nature*, 518(7540):529–533, 2015.

Prokhorov, Danil V, Wunsch, Donald C, et al. Adaptive critic designs. *Neural Networks, IEEE Transactions on*, 8(5):997–1007, 1997.

Schulman, John, Heess, Nicolas, Weber, Theophane, and Abbeel, Pieter. Gradient estimation using stochastic computation graphs. In *Advances in Neural Information Processing Systems*, pp. 3510–3522, 2015a.

Schulman, John, Levine, Sergey, Moritz, Philipp, Jordan, Michael I, and Abbeel, Pieter. Trust region policy optimization. *arXiv preprint arXiv:1502.05477*, 2015b.

Silver, David, Lever, Guy, Heess, Nicolas, Degris, Thomas, Wierstra, Daan, and Riedmiller, Martin. Deterministic policy gradient algorithms. In *ICML*, 2014.

Tassa, Yuval, Erez, Tom, and Todorov, Emanuel. Synthesis and stabilization of complex behaviors through online trajectory optimization. In *Intelligent Robots and Systems (IROS), 2012 IEEE/RSJ International Conference on*, pp. 4906–4913. IEEE, 2012.

Todorov, Emanuel and Li, Weiwei. A generalized iterative lqg method for locally-optimal feedback control of constrained nonlinear stochastic systems. In *American Control Conference, 2005. Proceedings of the 2005*, pp. 300–306. IEEE, 2005.

Todorov, Emanuel, Erez, Tom, and Tassa, Yuval. Mujoco: A physics engine for model-based control. In *Intelligent Robots and Systems (IROS), 2012 IEEE/RSJ International Conference on*, pp. 5026–5033. IEEE, 2012.

Uhlenbeck, George E and Ornstein, Leonard S. On the theory of the brownian motion. *Physical review*, 36(5):823, 1930.

Wahlström, Niklas, Schön, Thomas B, and Deisenroth, Marc Peter. From pixels to torques: Policy learning with deep dynamical models. *arXiv preprint arXiv:1502.02251*, 2015.

Watkins, Christopher JCH and Dayan, Peter. Q-learning. *Machine learning*, 8(3-4):279–292, 1992.

Wawrzyński, Paweł. Real-time reinforcement learning by sequential actor–critics and experience replay. *Neural Networks*, 22(10):1484–1497, 2009.

Wawrzyński, Paweł. Control policy with autocorrelated noise in reinforcement learning for robotics. *International Journal of Machine Learning and Computing*, 5:91–95, 2015.

Wawrzyński, Paweł and Tanwani, Ajay Kumar. Autonomous reinforcement learning with experience replay. *Neural Networks*, 41:156–167, 2013.

Supplementary Information: Continuous control with deep reinforcement learning

7 EXPERIMENT DETAILS

We used Adam (Kingma & Ba, 2014) for learning the neural network parameters with a learning rate of 10^{-4} and 10^{-3} for the actor and critic respectively. For Q we included L_2 weight decay of 10^{-2} and used a discount factor of $\gamma = 0.99$. For the soft target updates we used $\tau = 0.001$. The neural networks used the rectified non-linearity (Glorot et al., 2011) for all hidden layers. The final output layer of the actor was a $\tanh$ layer, to bound the actions. The low-dimensional networks had 2 hidden layers with 400 and 300 units respectively ($\approx$ 130,000 parameters). Actions were not included until the 2nd hidden layer of Q. When learning from pixels we used 3 convolutional layers (no pooling) with 32 filters at each layer. This was followed by two fully connected layers with 200 units ($\approx$ 430,000 parameters). The final layer weights and biases of both the actor and critic were initialized from a uniform distribution $[-3 \times 10^{-3}, 3 \times 10^{-3}]$ and $[3 \times 10^{-4}, 3 \times 10^{-4}]$ for the low dimensional and pixel cases respectively. This was to ensure the initial outputs for the policy and value estimates were near zero. The other layers were initialized from uniform distributions $[-\frac{1}{\sqrt{f}}, \frac{1}{\sqrt{f}}]$ where f is the fan-in of the layer. The actions were not included until the fully-connected layers. We trained with minibatch sizes of 64 for the low dimensional problems and 16 on pixels. We used a replay buffer size of 10^6.

For the exploration noise process we used temporally correlated noise in order to explore well in physical environments that have momentum. We used an Ornstein-Uhlenbeck process (Uhlenbeck & Ornstein, 1930) with $\theta = 0.15$ and $\sigma = 0.2$. The Ornstein-Uhlenbeck process models the velocity of a Brownian particle with friction, which results in temporally correlated values centered around 0.

8 PLANNING ALGORITHM

Our planner is implemented as a model-predictive controller (Tassa et al., 2012): at every time step we run a single iteration of trajectory optimization (using iLQG, (Todorov & Li, 2005)), starting from the true state of the system. Every single trajectory optimization is planned over a horizon between 250ms and 600ms, and this planning horizon recedes as the simulation of the world unfolds, as is the case in model-predictive control.

The iLQG iteration begins with an initial rollout of the previous policy, which determines the nominal trajectory. We use repeated samples of simulated dynamics to approximate a linear expansion of the dynamics around every step of the trajectory, as well as a quadratic expansion of the cost function. We use this sequence of locally-linear-quadratic models to integrate the value function backwards in time along the nominal trajectory. This *back-pass* results in a putative modification to the action sequence that will decrease the total cost. We perform a derivative-free line-search over this direction in the space of action sequences by integrating the dynamics forward (the *forward-pass*), and choose the best trajectory. We store this action sequence in order to warm-start the next iLQG iteration, and execute the first action in the simulator. This results in a new state, which is used as the initial state in the next iteration of trajectory optimization.

9 ENVIRONMENT DETAILS

9.1 TORCS ENVIRONMENT

For the Torcs environment we used a reward function which provides a positive reward at each step for the velocity of the car projected along the track direction and a penalty of -1 for collisions. Episodes were terminated if progress was not made along the track after 500 frames.

9.2 MuJoCo environments

For physical control tasks we used reward functions which provide feedback at every step. In all tasks, the reward contained a small action cost. For all tasks that have a static goal state (e.g. pendulum swingup and reaching) we provide a smoothly varying reward based on distance to a goal state, and in some cases an additional positive reward when within a small radius of the target state. For grasping and manipulation tasks we used a reward with a term which encourages movement towards the payload and a second component which encourages moving the payload to the target. In locomotion tasks we reward forward action and penalize hard impacts to encourage smooth rather than hopping gaits (Schulman et al., 2015b). In addition, we used a negative reward and early termination for falls which were determined by simple threshholds on the height and torso angle (in the case of walker2d).

Table 2 states the dimensionality of the problems and below is a summary of all the physics environments.

task name	$\dim(\mathbf{s})$	$\dim(\mathbf{a})$	$\dim(\mathbf{o})$
blockworld1	18	5	43
blockworld3da	31	9	102
canada	22	7	62
canada2d	14	3	29
cart	2	1	3
cartpole	4	1	14
cartpoleBalance	4	1	14
cartpoleParallelDouble	6	1	16
cartpoleParallelTriple	8	1	23
cartpoleSerialDouble	6	1	14
cartpoleSerialTriple	8	1	23
cheetah	18	6	17
fixedReacher	10	3	23
fixedReacherDouble	8	2	18
fixedReacherSingle	6	1	13
gripper	18	5	43
gripperRandom	18	5	43
hardCheetah	18	6	17
hardCheetahNice	18	6	17
hopper	14	4	14
hyq	37	12	37
hyqKick	37	12	37
movingGripper	22	7	49
movingGripperRandom	22	7	49
pendulum	2	1	3
reacher	10	3	23
reacher3daFixedTarget	20	7	61
reacher3daRandomTarget	20	7	61
reacherDouble	6	1	13
reacherObstacle	18	5	38
reacherSingle	6	1	13
walker2d	18	6	41

Table 2: Dimensionality of the MuJoCo tasks: the dimensionality of the underlying physics model $\dim(s)$, number of action dimensions $\dim(a)$ and observation dimensions $\dim(o)$.

task name	**Brief Description**
blockworld1	Agent is required to use an arm with gripper constrained to the 2D plane to grab a falling block and lift it against gravity to a fixed target position.

blockworld3da	Agent is required to use a human-like arm with 7-DOF and a simple gripper to grab a block and lift it against gravity to a fixed target position.
canada	Agent is required to use a 7-DOF arm with hockey-stick like appendage to hit a ball to a target.
canada2d	Agent is required to use an arm with hockey-stick like appendage to hit a ball initialzed to a random start location to a random target location.
cart	Agent must move a simple mass to rest at 0. The mass begins each trial in random positions and with random velocities.
cartpole	The classic cart-pole swing-up task. Agent must balance a pole attached to a cart by applying forces to the cart alone. The pole starts each episode hanging upside-down.
cartpoleBalance	The classic cart-pole balance task. Agent must balance a pole attached to a cart by applying forces to the cart alone. The pole starts in the upright positions at the beginning of each episode.
cartpoleParallelDouble	Variant on the classic cart-pole. Two poles, both attached to the cart, should be kept upright as much as possible.
cartpoleSerialDouble	Variant on the classic cart-pole. Two poles, one attached to the cart and the second attached to the end of the first, should be kept upright as much as possible.
cartpoleSerialTriple	Variant on the classic cart-pole. Three poles, one attached to the cart, the second attached to the end of the first, and the third attached to the end of the second, should be kept upright as much as possible.
cheetah	The agent should move forward as quickly as possible with a cheetah-like body that is constrained to the plane. This environment is based very closely on the one introduced by Wawrzyński (2009); Wawrzyński & Tanwani (2013).
fixedReacher	Agent is required to move a 3-DOF arm to a fixed target position.
fixedReacherDouble	Agent is required to move a 2-DOF arm to a fixed target position.
fixedReacherSingle	Agent is required to move a simple 1-DOF arm to a fixed target position.
gripper	Agent must use an arm with gripper appendage to grasp an object and manuver the object to a fixed target.
gripperRandom	The same task as `gripper` except that the arm object and target position are initialized in random locations.
hardCheetah	The agent should move forward as quickly as possible with a cheetah-like body that is constrained to the plane. This environment is based very closely on the one introduced by Wawrzyński (2009); Wawrzyński & Tanwani (2013), but has been made much more difficult by removing the stabalizing joint stiffness from the model.
hopper	Agent must balance a multiple degree of freedom monoped to keep it from falling.
hyq	Agent is required to keep a quadroped model based on the hyq robot from falling.

movingGripper	Agent must use an arm with gripper attached to a moveable platform to grasp an object and move it to a fixed target.
movingGripperRandom	The same as the movingGripper environment except that the object position, target position, and arm state are initialized randomly.
pendulum	The classic pendulum swing-up problem. The pendulum should be brought to the upright position and balanced. Torque limits prevent the agent from swinging the pendulum up directly.
reacher3daFixedTarget	Agent is required to move a 7-DOF human-like arm to a fixed target position.
reacher3daRandomTarget	Agent is required to move a 7-DOF human-like arm from random starting locations to random target positions.
reacher	Agent is required to move a 3-DOF arm from random starting locations to random target positions.
reacherSingle	Agent is required to move a simple 1-DOF arm from random starting locations to random target positions.
reacherObstacle	Agent is required to move a 5-DOF arm around an obstacle to a randomized target position.
walker2d	Agent should move forward as quickly as possible with a bipedal walker constrained to the plane without falling down or pitching the torso too far forward or backward.